


## ORIGINAL ARTICLE

# Actin-like protein 8 promotes cell proliferation, colony-formation, proangiogenesis, migration and invasion in lung adenocarcinoma cells

Shanwu Ma<sup>1\*</sup> , Xiaowei Wang<sup>2\*</sup>, Zhenrong Zhang<sup>3</sup> & Deruo Liu<sup>3</sup>

1 Department of Thoracic Surgery, Peking University China-Japan Friendship School of Clinical Medicine, Beijing, China

2 Department of Pathology, China-Japan Friendship Hospital, Beijing, China

3 Department of Thoracic Surgery, China-Japan Friendship Hospital, Beijing, China

## Keywords

ACTL8; angiogenesis; cell proliferation; lung adenocarcinoma; migration.

## Correspondence

Deruo Liu, Department of Thoracic Surgery, China-Japan Friendship Hospital, No.2, East Yinghua Street, Beijing 100029, China.

Tel: +86 138 0118 6957

Fax: +86 010 8420 6189

Email: deruoliu@vip.sina.com

\*These authors contributed equally to this work and are joint first authors.

Received: 1 September 2019;

Accepted: 25 October 2019.

doi: 10.1111/1759-7714.13247

Thoracic Cancer **11** (2020) 526–536

## Abstract

**Background:** Non-small cell lung cancer (NSCLC) is the leading cause of cancer-associated mortality worldwide of which lung adenocarcinoma (LUAD) is the most common. The identification of oncogenes and effective drug targets is the key to individualized LUAD treatment. Actin-like protein 8 (ACTL8), a member of the cancer/testis antigen family, is associated with tumor growth and patient prognosis in various types of cancer. However, whether ACTL8 is involved in the development of LUAD remains unknown. The aim of the present study was to demonstrate the role of ACTL8 in human LUAD cells.

**Methods:** The expression of ACTL8 in LUAD tissues and cell lines was assessed using immunohistochemistry and western blotting. Additionally, plasmids expressing ACTL8-specific short hairpin RNAs were used to generate lentiviruses which were subsequently used to infect A549 and NCI-H1975 human LUAD cells. Cell proliferation, migration, invasion and apoptosis, as well as cell cycle progression and the expression of protein markers of epithelial to mesenchymal transition were investigated. A549 cell tumor growth in nude mice was also examined.

**Results:** The results showed that ACTL8 was highly expressed in A549 and NCI-H1975 LUAD cell lines. Additionally, ACTL8-knockdown inhibited proliferation, colony formation, cell cycle progression, migration and invasion, and increased apoptosis in both cell lines. Furthermore, in vivo experiments in nude mice revealed that ACTL8-knockdown inhibited A549 cell tumor growth.

**Conclusion:** These results suggest that ACTL8 serves an oncogenic role in human LUAD cells, and that ACTL8 may represent a potential therapeutic target for LUAD.

## Key points

Our results suggest that ACTL8 serves an oncogenic role in human LUAD cells, and that ACTL8 may represent a potential therapeutic target for LUAD.

## Introduction

Lung cancer is one of the most prevalent malignant diseases worldwide, with high morbidity and mortality rates. Non-small cell lung cancer (NSCLC), a heterogeneous group of lung cancer subtypes, accounts for the majority of lung cancer cases. The group includes lung

adenocarcinoma (LUAD), lung squamous cell carcinoma and large cell carcinoma, among which LUAD is the most commonly occurring subtype.<sup>1</sup> The five-year survival rate of patients with NSCLC is reported to be only 17%, despite advances in the understanding of the mechanisms of lung cancer; additionally, combination therapy using surgical resection, chemotherapy, radiation and targeted

therapy has not significantly improved the five-year survival rate.<sup>2</sup>

With the recent development of molecular biotechnology, numerous tumor target antigens that are associated with the growth, progression and metastasis of NSCLC have been identified, such as epidermal growth factor receptor (EGFR), anaplastic lymphoma kinase (ALK), KRAS proto-oncogene, and GTPase (KRAS).<sup>3–6</sup> Cancer/testis antigens (CTAs) are tumor-associated antigens, of which there are >200 different types. CTAs are specifically and highly expressed in the placenta, various types of tumor tissues and the testicles, but low expression levels in normal tissue. They also promote immune responses in some cancer patients.<sup>7</sup> A number of CTAs, such as melanoma-associated antigen (MAGE-A) and New York esophageal squamous cell carcinoma 1 (NY-ESO-1), are prototype CTAs that elicit natural cellular immunity in cancers such as melanoma and ovarian, bladder and lung cancer. Both MAGE-A and NY-ESO-1 have entered the clinical trials stage, and the treatment of tumor patients has obtained good therapeutic results.<sup>8</sup>

ACTL8 is a member of the CTA family, and there are currently a limited number of studies focused on its association with tumors. Freitas *et al.* reported that ACTL8 was highly expressed in glioblastoma, but not associated with patient survival.<sup>9</sup> Furthermore, Yao *et al.* found that the expression level of ACTL8 was significantly increased in colon adenocarcinoma, breast cancer and endometrial carcinoma tissues.<sup>10</sup> However, the expression of ACTL8 in LUAD, and its relationship with the development and prognosis of the disease, remains undetermined. In order to investigate its potential role in LUAD, the expression levels of ACTL8 in lung adenocarcinoma tissues and cell lines were detected. Furthermore, the effects of ACTL8 on the function of A549 and NCI-H1975 cells were determined by short hairpin (sh) RNA-mediated ACTL8-knockdown. shACTL8 had a significant impact on proliferation, cell cycle progression, apoptosis, migration and invasion, angiogenesis and epithelial to mesenchymal transition (EMT) in A549 cells. Additionally, *in vivo* experiments in nude mice confirmed the results of the *in vitro* investigations, thus the present study demonstrated that ACTL8 may serve an important role and act as a potent oncoprotein in LUAD cells.

## Methods

### Expression levels of ACTL8 in the cancerous and paracancerous tumor tissues

The samples of LUAD, paracancerous, and normal tissue were obtained from the commercial tissue microarray (GeneChem Co., Ltd., Shanghai, China). The tissue

microarray was analyzed using immunohistochemistry (IHC) with an ACTL8 antibody. The experimental method was performed as previously described,<sup>11</sup> and the reagent for the detection of ACTL8 was purchased from Abcam (1:500; cat. no. ab96756).

### shRNA-ACTL8 design for lentivirus construction

shRNA-ACTL8 and the scramble shRNA-Ctrl were purchased from GeneChem Co., Ltd. (Shanghai, China). The experimental method was performed as previously described.<sup>12</sup> An shRNA sequence against the human ACTL8 target sequence (TGGAGATCCTGTTTGAGTT) was screened and transfected into 293T cells (GeneChem, Shanghai, China) to generate shRNA-ACTL8, while the shRNA-Ctrl was used as the negative control. The sequences of shRNA-ACTL8 and shRNA-Ctrl were GCTGGAGATCCTGTTTGAGTT and TTCTCCGAACGTGTCACGT, respectively.

### Cell culture and lentiviral infection

Cell lines including 10HBE, Beas-2B, HCC827, A549, H1299, NCI-H1975, 95-D, and PC-9 were purchased from the American Type Culture Collection and maintained in low passage culture as recommended. Briefly, the cells were cultured at 37°C (5% CO<sub>2</sub>) in F12K (A549 cells), DMEM (10HBE), BEBM (Beas-2B cells) or RPMI-1640 medium (NCI-H1975, H1299, HCC827, 95-D, and PC-9 cells) containing 10% fetal bovine serum (FBS) and 1% penicillin-streptomycin that were purchased from Gibco (Gibco, CA, USA). Both cell lines ( $2 \times 10^5$ ) were seeded into 6-well plates and infected with shRNA-ACTL8 or shRNA-Ctrl lentiviruses ( $5 \times 10^8$  TU/mL, 12  $\mu$ L); 72 hours post-infection, the mRNA and protein expression levels of ACTL8 were determined, and the cells subjected to functional analysis.

### Western blotting

Cells from each cell line were harvested and lysed, and the total protein extracted using RIPA buffer (Beyotime, Shanghai, China). The protein was then quantified using bicinchoninic acid Protein Assay kit (Beyotime, Shanghai, China). Denatured protein samples (20  $\mu$ g per lane) were separated by SDS-PAGE using a 10% gel, and transferred to PVDF membranes (EMD Millipore). The membranes were blocked with 5% skim milk for one hour at room temperature, and incubated with primary antibodies against ACTL8 (1:500; cat. no. ab96756; Abcam), N-cadherin (1:1000; cat. no. 4061; Cell Signaling Technology, Inc.), E-cadherin (1:1000; cat. no. 3195; Cell Signaling Technology, Inc.), vimentin (1:2000; cat. no. ab92547;

Abcam),  $\beta$ -catenin (1:1000; cat. no. 9562; Cell Signaling Technology, Inc.), apoptosis regulator BAX (1:2000; cat. no. ab53154; Abcam), caspase 3 (1:1000; cat. no. ab49822; Abcam) and GAPDH (1:2500; cat. no. sc-32 233; Santa-Cruz Biotechnology, Inc.). After washing three times in PBST (1  $\times$  PBS, 0.1% Tween 20), the membranes were further incubated with secondary antibodies (1:2000) for 1.5 hours at room temperature (HRP-conjugated anti-rabbit IgG, sc-2004, Santa-Cruz; HRP-conjugated anti-mouse IgG, sc-2005, Santa-Cruz). All blots were visualized using Pierce ECL Western Blotting Substrate kit (Thermo Fisher Scientific, CA, USA).

### Reverse transcription-quantitative (RT-q) PCR

Following lentiviral infection for 72 hours, total RNA was extracted from A549 and NCI-H1975 cells using TRIzol reagent (Invitrogen; Thermo Fisher Scientific, Inc.) and reverse transcribed using the PrimeScript RT reagent kit (Takara Biotechnology Co., Ltd.) according to the manufacturer's protocol. GAPDH was used as the endogenous control. qPCR analysis was performed using the TaqMan Universal PCR Master Mix on an ABI 7900HT Real-Time PCR system (both Applied Biosystems) using the following primers: ACTL8 forward, 5'-GAACATCGTGAACCTACCTACCG-3', and reverse, 5'-CAAGGGTGTCTC CGTGATGAT-3'; GAPDH forward, 5'-TGACTTCA ACAGCGACACCCA-3', and reverse, 5'-CACCTGTTG CTGTAGCCAAA -3'). The thermal cycling parameters were as follows: 95°C for 30 seconds, 40 cycles of 95°C for five seconds and 60°C for 30 seconds, and one cycle of 95°C for 15 seconds, 60°C for 30 seconds and 95°C for 15 seconds. Data were analyzed using the comparative CT method.

### Cellular proliferation analysis

Following lentiviral infection for 72 hours, A549 and NCI-H1975 cells were trypsinized, resuspended in complete medium and seeded into 96-well plates (2000 cell/well). The number of GFP-positive cells was detected using the Celigo cell counting system (Nexcelom Bioscience, Lawrence, MA, USA), every day for five consecutive days, and a cell proliferation curve was subsequently generated.

### Flow cytometric analysis

Lentivirus-infected cells (about  $1 \times 10^6$  cells) were washed with PBS and then resuspended in FACS buffer. The cells were stained with annexin V-APC, and an apoptosis detection kit (cat. 88-8007, eBioscience, CA, USA) was used to determine the percentage of apoptotic cells between the

different experimental groups, according to the manufacturer's instructions. Cell cycle progression was evaluated using propidium iodide (PI) alone. The cells were analyzed using a Guava easyCyte HT (Millipore, MA, USA).

### Colony-formation assay

After infection, A549 and NCI-H1975 cells were cultured for another 72 hours and harvested, and then resuspended in F12K (A549 cells) or RPMI-1640 medium (NCI-1975 cells) containing 10% FBS and seeded into 6-well plates (400 cells/well). The plates were cultured for 10 days in a 5% CO<sub>2</sub> incubator at 37°C and colonies with >50 cells were counted. The medium was changed every three days. Cells were then washed with PBS and fixed with 4% paraformaldehyde for 40 minutes. Cell colony was stained with Giemsa solution (ECM550, chemicon, MA, USA) for 20 minutes. The number of cell colonies was then manually counted using a light microscope (Olympus, Narishige, Japan).

### TUNEL (terminal deoxynucleotide transferase dUTP nick end labeling) assay

TUNEL assays were performed using the One Step TUNEL Apoptosis Assay kit (Beyotime, Shanghai, China) following the manufacturer's protocol. Briefly, infected A549 and NCI-H1975 cells were plated in 6-well plates ( $1 \times 10^6$  cells/well), fixed with 4% paraformaldehyde for 40 minutes at room temperature, and then incubated in the dark with TUNEL reagent for one hour at 37°C. The cells were counterstained with DAPI dissolved in PBS, and the condensed or fragmented nuclei were observed using a fluorescence microscope (Olympus, Narishige, Japan).

### Endothelial cell tube formation assay

The tube formation assay was conducted as described previously.<sup>13</sup> Briefly, following lentiviral infection, A549 and NCI-H1975 cells ( $2 \times 10^5$  cells/well) were cultured in complete growth medium until adherent. After being washed with D-Hanks twice, cells were then cultured in serum-free RPMI-1640 for an additional 24 hours. Cell suspension was collected. A total of 70  $\mu$ L of cold Matrigel was then transferred into each well of a 96-well plate and incubated at 37°C for 30 minutes. Human umbilical vein endothelial cells (HUVEC) were digested and washed with serum-free RPMI-1640. The HUVEC were then plated into the Matrigel-coated 96-well plates ( $2 \times 10^4$  cells per well) and treated with the cell suspension. The assay plate was incubated at 37°C for six hours. Tubes were subsequently stained with 2  $\mu$ M Calcein-AM for 20 minutes. Images were taken using a Celigo Imaging Cytometer (Nexcelom Bioscience, Lawrence, MA, USA).

## Wound healing assay

Following lentiviral infection, A549 and NCI-H1975 cells ( $5 \times 10^4$  cells/well) were cultured in complete growth medium until 90% confluency. Cell monolayer was scraped with a 10  $\mu$ L pipette tip to generate wounds and washed twice with serum-free RPMI-1640. Cells were then cultured in RPMI-1640 (0.5% FBS) for an additional 48 hours. Images were taken at 0 and 24 hours to visualize wound healing.

## Cell migration assay

Following lentiviral infection, A549 and NCI-H1975 cells ( $5 \times 10^4$  cells/well) were seeded into the upper chamber of Transwell inserts with 500  $\mu$ L serum-free RPMI-1640; the inserts contained a 8  $\mu$ m pore size membrane with a thin layer Matrigel matrix. The lower chamber was filled with 700  $\mu$ L RPMI-1640 (20% FBS). After 48 hours at 37°C, cells that had penetrated the membrane were fixed and stained with Giemsa solution (ECM550, chemicon, MA, USA) for 20 minutes at room temperature. The number of invasive cells was then counted using a light microscope (Olympus, Narishige, Japan).

## Imaging assay

Luciferase-positive A549 cells were infected with shACTL8 or shCtrl lentiviruses;  $1 \times 10^7$  cells were resuspended in 200  $\mu$ L PBS and injected subcutaneously into six-week-old female BALB/c nu/nu mice (about 20 g) obtained from Shanghai SLAC Laboratory Animal Co., Ltd (Shanghai, China). The animals were housed at  $25 \pm 2^\circ\text{C}$  at a relative humidity of  $50 \pm 10\%$  under natural light/dark conditions. Food and water were sterilized and freely available. After four weeks, a IVIS Lumina LT SERIES III (PerkinElmer, CA, USA) was used to investigate the malignant progress of transplanted tumor cells by bioluminescence imaging. All of the images were taken 15 minutes after intraperitoneal injection of D-luciferin (15 mg/mL) (Sigma-Aldrich, MO, USA) of 10 mL/kg bodyweight. The mice were euthanized with CO<sub>2</sub> (10%/minute), and complete euthanasia was judged by cessation of heart beat and breathing. The tumors were then resected and weighed. All animal experiments were approved by the Animal Care and Welfare Committee of the China-Japan Friendship Hospital (170205).

## Hematoxylin and eosin (H&E) staining

The tumor tissues from nude mice were fixed in 4% paraformaldehyde overnight at 4°C, and then embedded in paraffin. Sections (5  $\mu$ m thick) were cut, dewaxed and

hydrated. The sections were counterstained with hematoxylin and eosin, and observed under a light microscope (Olympus, Narishige, Japan).

## Statistical analysis

The data are presented as the mean  $\pm$  standard deviation relative to the control values. The statistical differences between the two experimental groups were determined using the unpaired Student's *t*-test. One-way ANOVA and Bonferroni tests were used to compare the expression levels of ACTL8 in tissues. The data were analyzed using GraphPad Prism v5.0 (GraphPad, San Diego, CA, USA), and  $P < 0.05$  was considered to indicate a statistically significant difference.

## Results

### ACTL8 is highly expressed in human LUAD tissues and lung cancer cell lines

The expression levels of ACTL8 in LUAD and paracancerous tissues were characterized in situ. The IHC scores were calculated and used to determine ACTL8 expression. A higher ACTL8 expression level was observed in the LUAD tissues compared with the paracancerous and normal lung tissues (Fig. 1(a) and (b)). Additionally, the expression levels of ACTL8 in six kinds of lung cancer cell line (HCC827, A549, H1299, NCI-H1975, 95-D and PC-9) were detected by western blotting, and a higher expression level was observed than in normal human bronchial epithelial cell lines (10HBE and Beas-2B; Fig. 1(c) and (d)). Among the cancerous cell lines, the expression levels of ACTL8 were the greatest in A549 and NCI-H1975 cells.

### shRNA inhibition of ACTL8 reduces human LUAD cell proliferation

Given the oncogenic role of ACTL8 in the progression of breast cancer (10), the present study aimed to investigate the regulatory role of ACTL8 in NSCLC cell survival. A lentiviral knockdown system was employed to silence endogenous ACTL8 protein expression in A549 and NCI-H1975 cells (Fig. 2). The ability of shACTL8 to reduce cancer cell proliferation, and the subsequent effects on cell cycle progression were determined by using Celigo and flow cytometry assays. As shown in Figure 3(a) and (b), A549 and NCI-H1975 cell proliferation was markedly decreased in response to shACTL8, compared with the shRNA negative control.

To determine the effects of shACTL8 on cell cycle progression in lung cancer, A549 and NCI-H1975 cells were treated with lenti-shCtrl and lenti-shACTL8. The cells were

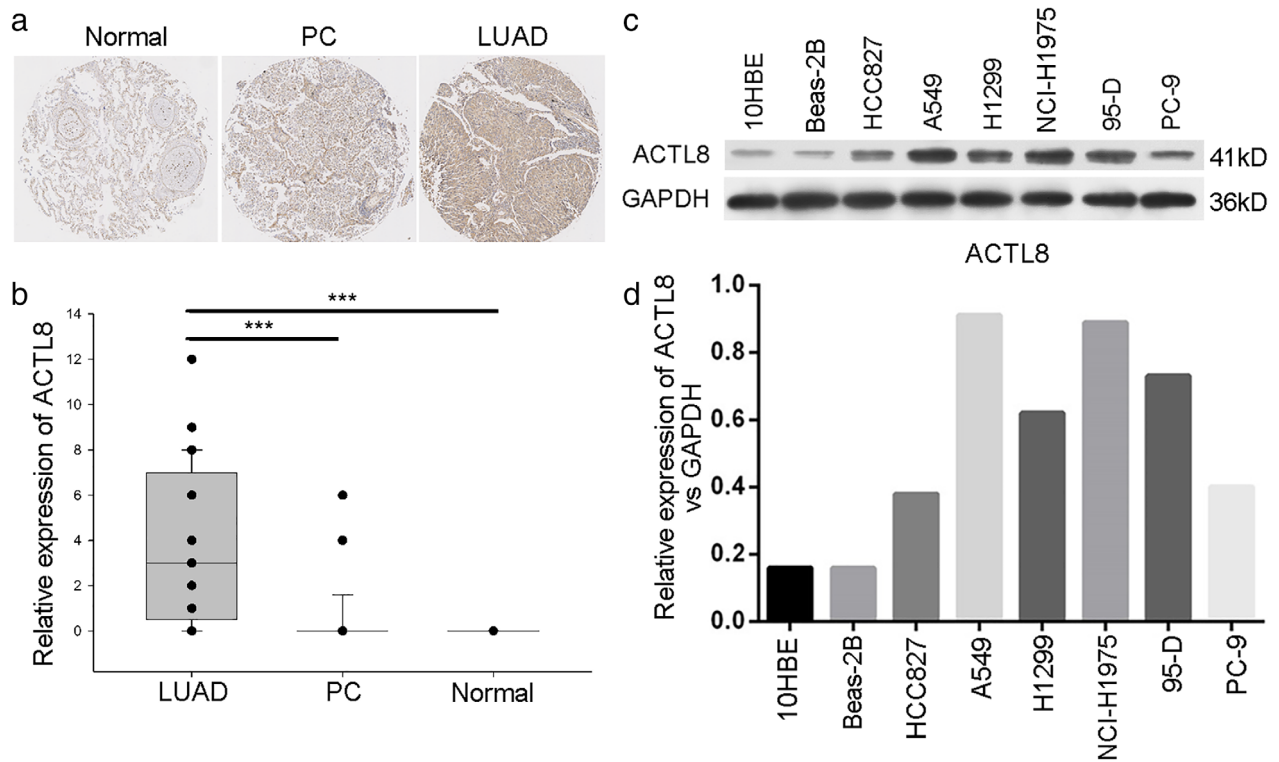


**Figure 1** High expression levels of ACTL8 in LUAD tissues and lung cancer cells. (a) LUAD ( $n = 45$ ), PC ( $n = 45$ ), and normal ( $n = 10$ ) tissues were prepared for IHC. (b) IHC analysis was scored according to the above mentioned methods. The data are presented as the mean  $\pm$  standard deviation;  $***P < 0.001$ . (c and d) Protein expression levels of ACTL8 were determined using western blotting in HCC827, A549, H1299, NCI-H1975, 95-D and PC-9 lung cancer cell lines. 10HBE and Beas-2B normal human bronchial epithelial cells were used as the controls. ACTL8, Actin-like protein 8; LUAD, lung adenocarcinoma; PC, paracancerous; IHC, immunohistochemistry.

stained with PI and subsequently analyzed using flow cytometry. As shown in Figure 3(c) and (d), lenti-shACTL8 resulted in an increase in the  $G_1$  population of 6.97% in A549 and 5.52% in NCI-H1975 cells. Consequently, the number of cells in the S phase was decreased, and that in the  $G_2/M$  phase was increased in the lenti-shACTL8 group (Fig. 3(c) and (d)).

**shRNA inhibition of ACTL8 promotes human LUAD cell apoptosis**

Since a reduction in cell proliferation was induced by shACTL8, it was hypothesized that this may be attributed to an increase in apoptosis, which was determined using annexin V/PI staining and flow cytometry. A significant increase in apoptosis was observed in lenti-shACTL8 A549 and NCI-H1975 cells three days' post-infection. Compared with that of the shCtrl group, the proportion of apoptotic cells increased from 3.59% to 8.09% in A549, and from 4.9% to 22.89% in NCI-H1975 cells following lenti-shACTL8 treatment (Fig. 4(a)). In addition, a TUNEL assay revealed that cleaved DNA, a hallmark indication of apoptosis, was observed in both cell lines infected with

lenti-shACTL8 (Fig. 4(b)). Furthermore, the expression levels of caspase 3 and BAX were increased in both cell lines infected with lenti-shACTL8 (Fig. 4(c)). These findings suggest that ACTL8 shRNA-mediated downregulation of A549 and NCI-H1975 cell proliferation was partially due to the induction of apoptosis.

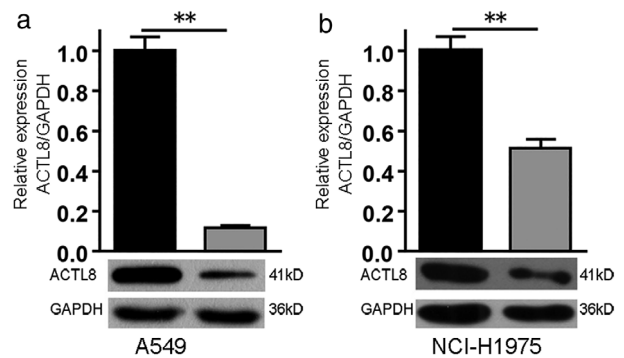
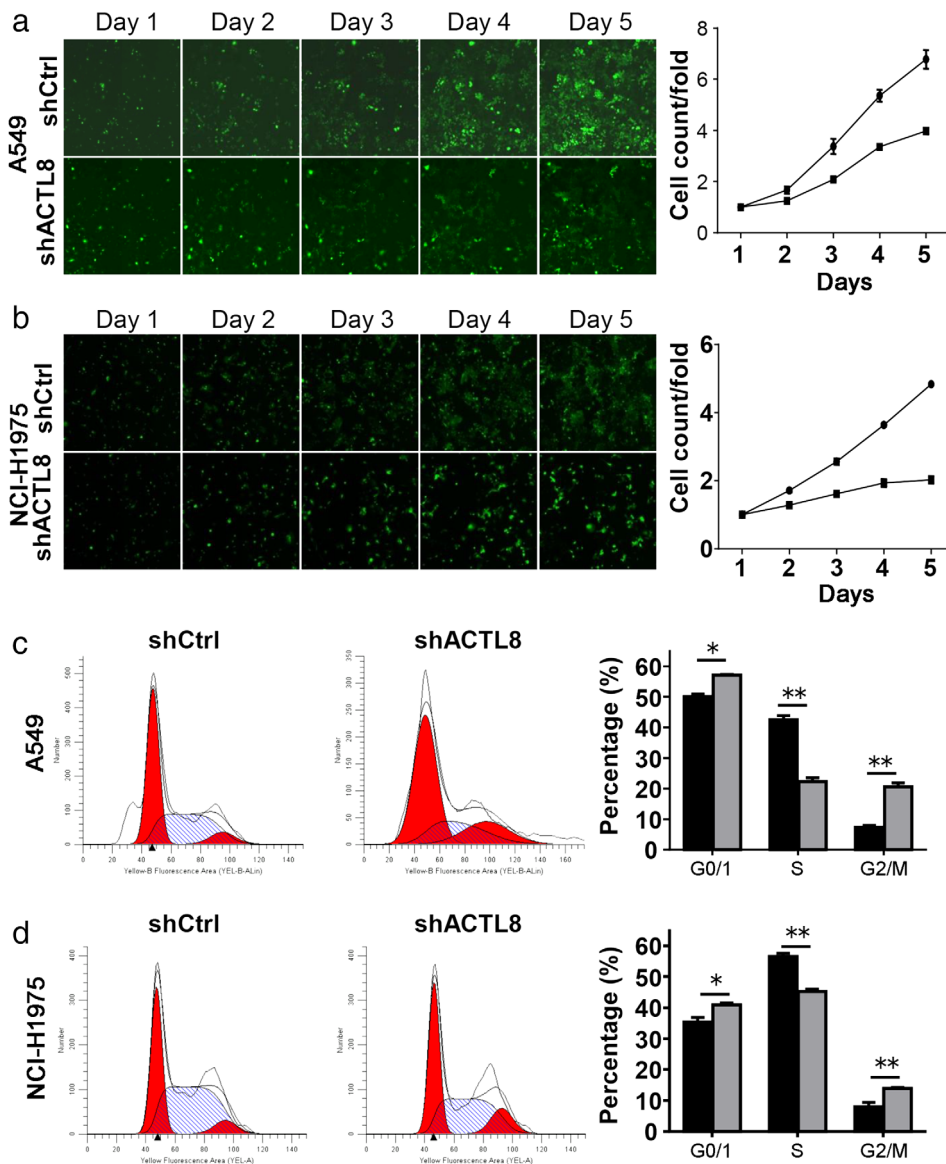


**Figure 2** shACTL8 lentivirus decreases the mRNA and protein expression levels of ACTL8. Expression of the ACTL8 gene at the mRNA and protein level in A549 (a) and NCI-H1975 (b) cells.  $**P < 0.01$ . ACTL8, Actin-like protein 8; sh, short-hairpin. (■) shCtrl and (▒) shACTL8.

**Figure 3** ACTL8 promotes human LUAD cell proliferation. (a) A549 and NCI-H1975 cell counts using the Celigo cell counting system. (b) Cells were infected with lenti-shACTL8 and lenti-shCtrl for three days, and proliferation was assessed every day for five consecutive days. (—●—) shCtrl and (—■—) shACTL8. (c) Flow cytometric analysis of A549 and NCI-H1975 cells (d) three days after infection; the number of cells in the G<sub>0</sub>/G<sub>1</sub> phase was increased, the number in the S phase was decreased, and the number in the G<sub>2</sub>/M phase was increased in the lenti-shACTL8 group, compared with the control group. (■) shCtrl and (▣) shACTL8. The data are presented as the mean ± standard deviation;  $n = 3$ . \* $P < 0.05$  and \*\* $P < 0.01$  versus lenti-shCtrl. ACTL8, Actin-like protein 8; LUAD, lung adenocarcinoma; sh, short-hairpin; lenti, lentivirus; Ctrl, control.



### shRNA inhibition of ACTL8 reduces the colony-forming ability of human LUAD cells

The role of ACTL8 in the regulation of colony formation was investigated. Lenti-shACTL8 was found to significantly suppress the colony-forming ability of A549 and NCI-H1975 cells (Fig. 5), demonstrating that ACTL8 is able to promote colony formation and cell viability.

### ACTL8 promotes angiogenesis in human LUAD cells

To determine the effect of ACTL8 on angiogenesis, tube formation assay was conducted using A549 and NCI-

H1975 cells infected with lenti-shACTL8 or lenti-shCtrl. The results showed that lenti-shACTL8 significantly reduced the tube formation of A549 cells compared with lenti-shCtrl (Fig. 6(a)). However, lenti-shACTL8 had no effect in the NCI-H1975 cells (Fig. 6(b)). These results suggested that ACTL8 had a proangiogenic effect on A549 cells, and that this effect was cell line-dependent.

### shRNA inhibition of ACTL8 reduces the migration and invasion abilities of human LUAD cells

The effect of ACTL8 inhibition on cancer cell migration and invasion were also evaluated using Transwell and Matrigel

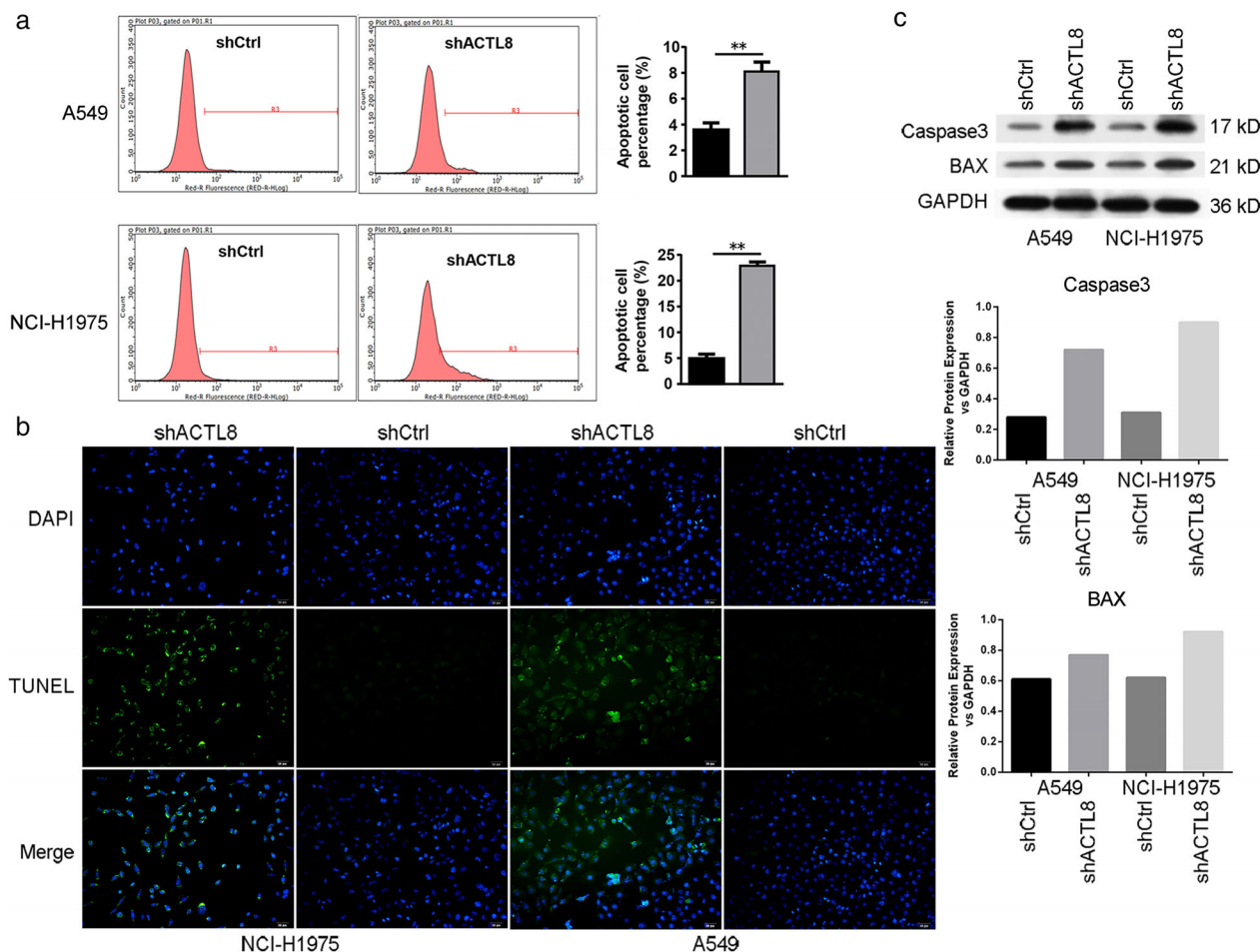


**Figure 4** ACTL8 regulates human LUAD cell apoptosis. (a) The percentage of apoptotic A549 and NCI-H1975 cells was measured using flow cytometry, and the number of apoptotic cells was significantly increased in the lenti-shACTL8 groups. The apoptotic rate was calculated as the percentage of FITC-positive cells. The data are presented as the mean ± standard deviation; n = 3. \*\*P < 0.01 versus lenti-shCtrl. (■) shCtrl and (▣) shACTL8. (b) Apoptotic A549 and NCI-H1975 cells were assessed using a TUNEL assay (magnification, 200x). (c) The expression of apoptosis-related proteins apoptosis regulator BAX and Caspase 3 was determined by western blotting, and GAPDH was used as the loading control. ACTL8, Actin-like protein 8; LUAD, lung adenocarcinoma; sh, short-hairpin; lenti, lentivirus; Ctrl, control.

assays, respectively. Figure 7(a) and (b) demonstrate that lenti-shACTL8 decreased the migrational capacity of NCI-H1975 cells, but had no effect on that of the A549 cells. However, downregulation of ACTL8 significantly suppressed the invasion abilities of both A549 and NCI-H1975 cells (Fig. 7(c) and (d) with or without Matrigel (Fig. 7(e) and (f)). The results suggest that shRNA knockdown of ACTL8 significantly suppresses lung cancer cell invasion.

**shRNA inhibition of ACTL8 reduces EMT in human LUAD cells**

EMT serves a key role in the metastasis of LUAD.<sup>14</sup> Tumor progression is often associated with the loss of E-cadherin and β-catenin, and an increase in the expression levels of vimentin and N-cadherin, which result in more motile

and invasive characteristics.<sup>15</sup> To investigate the effect of lenti-shACTL8 on E-cadherin, β-catenin, vimentin and N-cadherin, A549 and NCI-H1975 cells were infected with lenti-shACTL8 for three days and evaluated by western blotting. It was revealed that shACTL8 significantly increased the expression level of N-cadherin and β-catenin, and decreased that of vimentin in A549 cells. However, an increase of N-cadherin was observed in NCI-H1975 cells (Fig. 8). These data suggest that ACTL8 may promote the EMT of A549 cells, and that this effect was cell line-dependent.

**shRNA inhibition of ACTL8 reduces tumor burden in vivo**

Considering the inhibitory effects of ACTL8 knockdown on tumor cell proliferation, migration, invasion and EMT

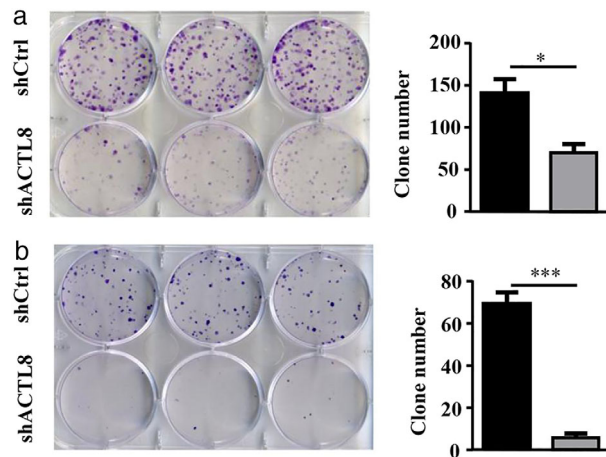


**Figure 5** ACTL8 regulates the colony-forming ability of human LUAD cells. (a) Colony-formation assays were performed using A549 cells following infection with lenti-shACTL8 or lenti-shCtrl. (b) The colony-forming ability of NCI-H1975 cells following transfection with lenti-shACTL8 or lenti-shCtrl. The data are presented as the mean  $\pm$  standard deviation;  $n = 3$ . \* $P < 0.05$  and \*\*\* $P < 0.001$  vs. lenti-shCtrl. ACTL8, Actin-like protein 8; LUAD, lung adenocarcinoma; sh, short-hairpin; lenti, lentivirus; Ctrl, control. (■) shCtrl and (□) shACTL8.

in vitro, it was hypothesized that shACTL8 may also inhibit tumor development in vivo. Therefore, nude mice were subcutaneously injected with lentivirus-infected, luciferase-positive A549 cells to induce tumor formation. As determined by bioluminescence (Fig. 9(a) and (b)), all mice injected with luciferase-positive A549 cells developed tumor four weeks after injection. In the lenti-shACTL8 group, the bioluminescence signals of the tumors were reduced (maximum diameter, 1.7 cm), compared with those of the lenti-shCtrl group (maximum diameter, 1.9 cm), implicating that tumor growth arrest was induced by shACTL8. The change in tumor weight also confirmed this phenomenon (Fig. 9(c)). Furthermore, H&E staining of the tumor tissues showed the typical structural features of LUAD in the shACTL8 and shCtrl groups (Fig. 9(d)). Thus, the results indicated that ACTL8 knockdown reduced LUAD tumor burden in mice.

## Discussion

LUAD is the most commonly diagnosed subtype of lung cancer, which is one of the most prevalent malignant diseases worldwide.<sup>1</sup> The five-year survival rate of patients has not substantially improved, despite considerable advances in our understanding of the molecular nature of lung cancer, and the use of combined therapy, including surgical resection, chemotherapy, radiation and targeted therapy.<sup>2</sup> Therefore, the investigation and identification of novel therapeutic targets is of great importance.

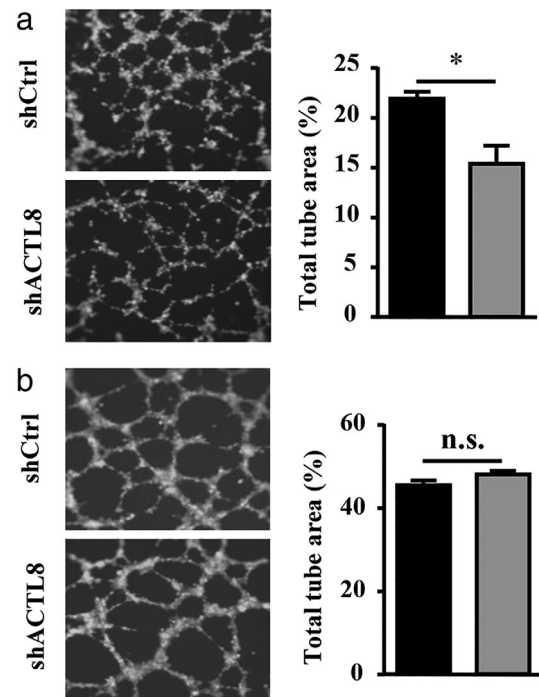


**Figure 6** ACTL8 regulates angiogenesis in human LUAD cells. (a) Infection with lenti-shACTL8 for 24 hours abolished the A549 cell-induced increase in tube formation. (b) Infection with lenti-shACTL8 for 24 hours had no effect on the NCI-H1975-induced increase in tube formation. The area of the tube branches was calculated and quantified. The data are presented as the mean  $\pm$  standard deviation;  $n = 3$ . \* $P < 0.05$  and \*\*\* $P < 0.001$  versus lenti-shCtrl. ACTL8, Actin-like protein 8; LUAD, lung adenocarcinoma; sh, short-hairpin; lenti, lentivirus; Ctrl, control. (■) shCtrl and (□) shACTL8.

CTA family members have become increasingly recognized as promising targets for cancer immunotherapy,<sup>16,17</sup> and are considered to be targets of the immune response in breast cancer and myeloma.<sup>17,18</sup> Within the CTA family, MAGEA and NY-ESO-1/CTAG1B have been used in clinical trials for lung cancer and melanoma.<sup>19,20</sup> Moreover, a monoclonal antibody against ACTL4 (Ipilimumab) has been used in the clinical trial stage.<sup>21</sup> As a member of the CTA family, the expression level of ACTL8 was shown to be significantly increased in colon adenocarcinoma, breast cancer and endometrial carcinoma tissues, compared with that in normal tissues.<sup>10</sup> Li *et al.*<sup>22</sup> demonstrated that high expression levels of ACTL8 were associated with poor patient prognosis and accelerated tumor progression in head and neck squamous cell carcinoma. However, the relationship between ACTL8 and the development of LUAD remains unclear. Therefore, the present study investigated the expression levels of ACTL8 in LUAD, and to the best of our knowledge, is the first to describe the anti-cancer effects of ACTL8 inhibition on the proliferation, cell cycle progression, apoptosis, migration and invasion,



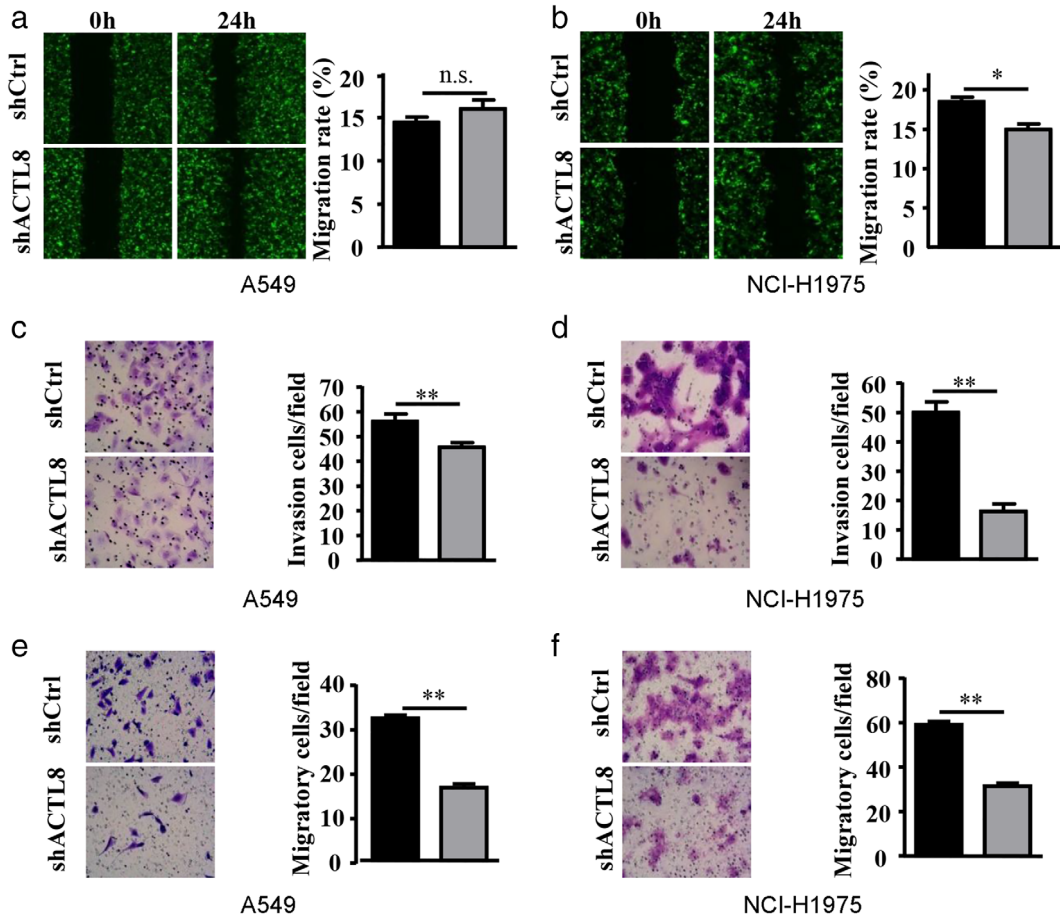


**Figure 7** ACTL8 regulates the migration and invasion of human LUAD cells. Wound-closure experiments were conducted using A549 and NCI-H1975 cells infected with lenti-shACTL8 or lenti-shCtrl. (a and b) Images were captured at 0 and 24 hours (left), and the relative cell migration was analyzed by comparison to the relative change in the wound-space distance (right) of A549 and NCI-H1975 cells. Invaded (c and e) A549 and (d and f) NCI-H1975 cells were assessed using Transwell assays with Matrigel (c and d) or without Matrigel (e and f), stained with Giemsa, and relative cell invasion was determined. The data are presented as the mean ± standard deviation; n = 3. \*P < 0.05 and \*\*P < 0.01 versus lenti-shCtrl. ACTL8, Actin-like protein 8; LUAD, lung adenocarcinoma; sh, short-hairpin; lenti, lentivirus; Ctrl, control. (■) shCtrl and (□) shACTL8.

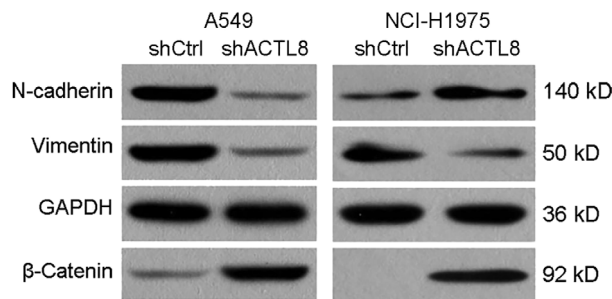


**Figure 8** ACTL8 regulates the epithelial to mesenchymal transition of human LUAD cells. A549 and NCI-H1975 cells were infected with lenti-shACTL8 or shCtrl for 72 hours, and the expression levels of N-cadherin, Vimentin and β-Catenin were determined using western blotting. ACTL8, Actin-like protein 8; LUAD, lung adenocarcinoma; sh, short-hairpin; lenti, lentivirus; Ctrl, control.

angiogenesis and EMT of LUAD cell lines, and on tumor-forming activity in nude mice. However, although shACTL8 significantly increased the expression level of EMT-related proteins in A549 cells, it is not clear how ACTL8 regulates EMT-related proteins. This specific molecular mechanism needs further study.

In the present study, the expression of ACTL8 was analyzed in LUAD and paracancerous tissues, demonstrating that ACTL8 was highly expressed in human LUAD tissues. Lentiviral-shRNA knockdown of ACTL8 was also conducted, resulting in ACTL8 inhibition at the mRNA and protein levels. ACTL8 downregulation exerted marked effects on A549 and NCI-H1975 cell proliferation, cell cycle progression, apoptosis, migration and invasion, angiogenesis and EMT, compared with the negative control group. In addition, in vivo studies revealed that ACTL8

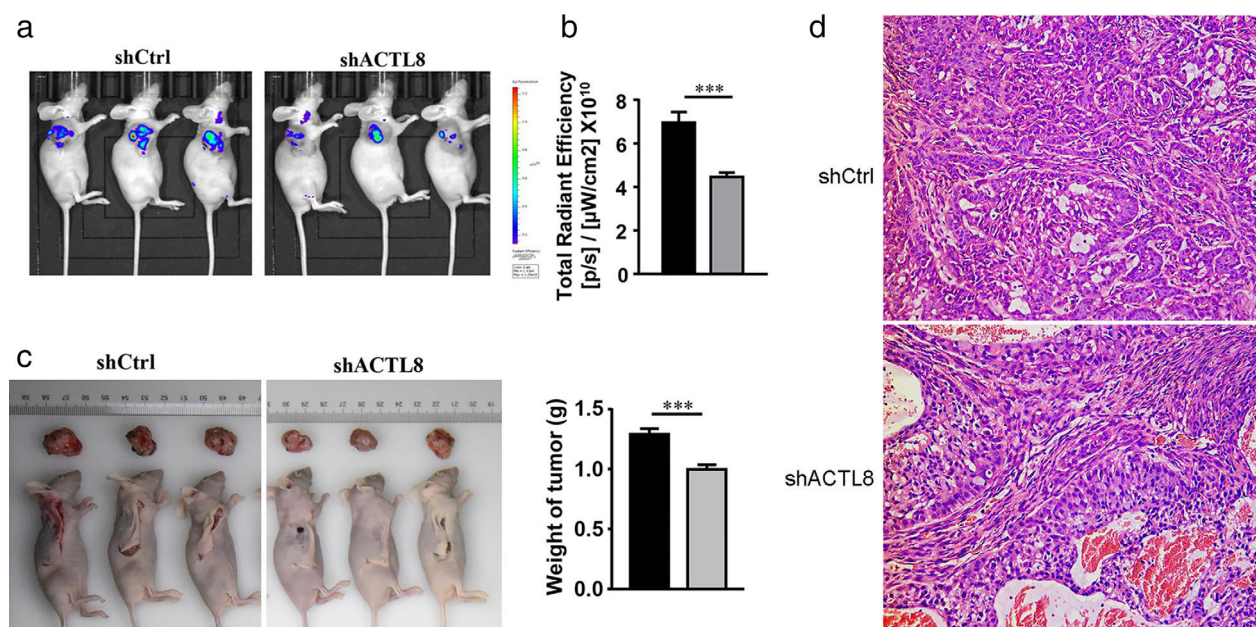


**Figure 9** shRNA inhibition of ACTL8 reduces tumor growth in vivo. Six-weeks-old female BALB/c nu/nu mice were subcutaneously injected with lentivirus-infected A549 cells. (a) Representative live images of the mice treated with A549 cells four weeks after inoculation. (b) Bioluminescence signals were analyzed and quantified using the Living Image 3.0 system four weeks post-inoculation. (c) Tumor weight change after cell injection. The data are presented as the mean  $\pm$  standard deviation;  $n = 10$ . \* $P < 0.05$  and \*\* $P < 0.01$  versus lenti-shCtrl. (■) shCtrl and (□) shACTL8. (d) H&E staining of the excised tumors (magnification,  $\times 200$ ). ACTL8, Actin-like protein 8; sh, short-hairpin; lenti, lentivirus; Ctrl, control.

knockdown reduced tumor growth. These results indicate that ACTL8 may be a potential candidate for the prevention of human LUAD development and metastasis.

With the development of molecular biotechnology, individualized and accurate molecular treatment programs are a potential future prospect, and numerous tumor target antigens have already been identified. These include EGFR, ROS1, BRAF, KRAS, HER2, c-MET, RET, PIK3CA, FGFR1 and DDR2,<sup>6</sup> which have given rise to new possibilities for targeted cancer therapy. Consistently, clinical trials have explored a number of these therapeutic targets, and when compared with conventional radiotherapy and chemotherapy, targeting these antigens comes with significantly improved survival benefits and considerable toxicity tolerance.<sup>18</sup> However, secondary drug resistance frequently occurs after a period of targeted therapy, resulting in decreased therapeutic effects and subsequent tumor progression.<sup>19</sup> EGFR mutations and ALK tyrosine kinase receptor fusions are frequently observed gene aberrations in LUAD, and the development of compounds against these targets has shown notable clinical benefit.<sup>20,23</sup> Nevertheless, drug resistance often occurs following treatment with tyrosine kinase inhibitors; according to related studies, this is primarily due to the T790M point mutation of the tyrosine kinase 20 exon, which results in the relative weakening of the ATP binding ability of EGFR-TKI. Drug

resistance is also influenced by factors such as c-MET gene amplification and GTPase KRas gene mutation.<sup>24</sup> It is therefore necessary to identify additional drug targets for the treatment of LUAD. The present study confirmed that downregulation of ACTL8 is an effective means of inhibiting LUAD, highlighting its downstream effectors as potential markers and therapeutic targets.

The present study demonstrated that the cancerous progression of A549 and NCI-H1975 cells, and their tumorigenic effects on nude mice were significantly inhibited by ACTL8 knockdown. Efficient delivery of a specific shRNA targeting ACTL8 or its downstream effectors may be used for further studies of lung cancer therapy. Thus, ACTL8 was revealed to be a potent oncoprotein in LUAD cells, and may serve as a potential biomarker and immunotherapeutic target for patients with LUAD.

## Disclosure

The authors declare that they have no competing interests.

## References

- 1 Siegel RL, Miller KD, Jemal A. Cancer statistics, 2019. *CA Cancer J Clin* 2019; **69**: 7–34.

- 2 Economopoulou P, Mountzios G. The emerging treatment landscape of advanced non-small cell lung cancer. *Ann Transl Med* 2018; **6**: 138.
- 3 Cafarotti S, Lococo F, Froesh P, Zappa F, Andre D. Target therapy in lung cancer. *Adv Exp Med Biol* 2016; **893**: 127–36.
- 4 Casaluze F, Sgambato A, Maione P et al. ALK inhibitors: A new targeted therapy in the treatment of advanced NSCLC. *Target Oncol* 2013; **8**: 55–67.
- 5 Singh M, Jadhav HR. Targeting non-small cell lung cancer with small-molecule EGFR tyrosine kinase inhibitors. *Drug Discov Today* 2018; **23**: 745–53.
- 6 Rothschild SI. Targeted therapies in non-small cell lung cancer-beyond EGFR and ALK. *Cancers (Basel)* 2015; **7**: 930–49.
- 7 Salmaninejad A, Zamani MR, Pourvahedi M et al. Cancer/testis antigens: Expression, regulation, tumor invasion, and use in immunotherapy of cancers. *Immunol Invest* 2016; **45**: 619–40.
- 8 Nishiyama T, Tachibana M, Horiguchi Y et al. Immunotherapy of bladder cancer using autologous dendritic cells pulsed with human lymphocyte antigen-A24-specific MAGE-3 peptide. *Clin Cancer Res* 2001; **7**: 23–31.
- 9 Freitas M, Malheiros S, Stavale JN et al. Expression of cancer/testis antigens is correlated with improved survival in glioblastoma. *Oncotarget* 2013; **4**: 636–46.
- 10 Yao J, Caballero OL, Yung WK et al. Tumor subtype-specific cancer-testis antigens as potential biomarkers and immunotherapeutic targets for cancers. *Cancer Immunol Res* 2014; **2**: 371–9.
- 11 Liu L, Li D, Chen S et al. B7-H4 expression in human infiltrating ductal carcinoma-associated macrophages. *Mol Med Rep* 2016; **14**: 2135–42.
- 12 Xu C, Sun L, Jiang C et al. SPPI, analyzed by bioinformatics methods, promotes the metastasis in colorectal cancer by activating EMT pathway. *Biomed Pharmacother* 2017; **91**: 1167–77.
- 13 Ucuzian AA, Greisler HP. In vitro models of angiogenesis. *World J Surg* 2007; **31**: 654–63.
- 14 Mou X, Liu S. MiR-485 inhibits metastasis and EMT of lung adenocarcinoma by targeting Flot2. *Biochem Biophys Res Commun* 2016; **477**: 521–6.
- 15 Zhu GJ, Song PP, Zhou H et al. Role of epithelial-mesenchymal transition markers E-cadherin, N-cadherin, beta-catenin and ZEB2 in laryngeal squamous cell carcinoma. *Oncol Lett* 2018; **15**: 3472–81.
- 16 Balafoutas D, zur Hausen A, Mayer S et al. Cancer testis antigens and NY-BR-1 expression in primary breast cancer: Prognostic and therapeutic implications. *BMC Cancer* 2013; **13**: 271.
- 17 Dhodapkar MV, Osman K, Teruya-Feldstein J et al. Expression of cancer/testis (CT) antigens MAGE-A1, MAGE-A3, MAGE-A4, CT-7, and NY-ESO-1 in malignant gammopathies is heterogeneous and correlates with site, stage and risk status of disease. *Cancer Immunol* 2003; **3**: 9.
- 18 Bria E, Bonomi M, Pilotto S et al. Clinical meta-analyses of targeted therapies in adenocarcinoma. *Target Oncol* 2013; **8**: 35–45.
- 19 Jackman D, Pao W, Riely GJ et al. Clinical definition of acquired resistance to epidermal growth factor receptor tyrosine kinase inhibitors in non-small-cell lung cancer. *J Clin Oncol* 2010; **28**: 357–60.
- 20 Gridelli C, Peters S, Sgambato A, Casaluze F, Adjei AA, Ciardiello F. ALK inhibitors in the treatment of advanced NSCLC. *Cancer Treat Rev* 2014; **40**: 300–6.
- 21 Postow MA, Luke JJ, Bluth MJ et al. Ipilimumab for patients with advanced mucosal melanoma. *Oncologist* 2013; **18**: 726–32.
- 22 Li B, Zhu J, Meng L. High expression of ACTL8 is poor prognosis and accelerates cell progression in head and neck squamous cell carcinoma. *Mol Med Rep* 2019; **19**: 877–84.
- 23 Khalil FK, Altiok S. Advances in EGFR as a predictive marker in lung adenocarcinoma. *Cancer Control* 2015; **22**: 193–9.
- 24 Crequit P, Ruppert AM, Rozensztajn N et al. EGFR and KRAS mutation status in non-small-cell lung cancer occurring in HIV-infected patients. *Lung Cancer* 2016; **96**: 74–7.